RNA (2001), *7*:182–193. Cambridge University Press. Printed in the USA.

The 100-kDa U5 snRNP protein (hPrp28p) contacts the 5′ splice site through its ATPase site

NAÏMA ISMAÏLI, MA SHA, E. HILARY GUSTAFSON, and MARIA M. KONARSKA
The Rockefeller University, New York, New York 10021, USA

ABSTRACT

To identify splicing factors in proximity of the 5′ splice site (5′SS), we followed a crosslinking profile of site-specifically modified, photoreactive RNA substrates. Upon U4/U5/U6 snRNP addition, the 5′SS RNA crosslinks in an ATP-dependent manner to U6 snRNA, an unidentified protein p27, and the 100-kDa U5 snRNP protein, a human ortholog of an ATPase/RNA helicase yPrp28p. The 5′SS:hPrp28p crosslink maps to the highly conserved TAT motif in proximity of the ATP-binding site in hPrp28p. We propose that hPrp28p acts as a helicase to unwind the 5′SS:U1 snRNA duplex, and at the same time as a 5′SS translocase, which, upon NTP-dependent conformational change, positions the 5′SS for pairing with U6 snRNA within the spliceosome. This repositioning of the 5′SS takes place regardless of whether the 5′SS is originally duplexed with U1 snRNA.

Keywords: 5′ splice site; pre-mRNA splicing, Prp28; RNA helicase; spliceosome

INTRODUCTION

Splicing of pre-mRNA involves two successive transesterification reactions carried out by a large ribonucleoprotein (RNP) spliceosome complex. This complex is composed of five snRNAs (U1, U2, U4, U5, and U6) and nearly 100 proteins (Moore et al., 1993). Spliceosome formation involves a complex network of specific and conserved interactions among snRNAs, as well as between snRNAs and pre-mRNA, that lead to formation of the catalytic center. During this process, an initial interaction of U1 snRNP with the 5′ splice site (5′SS) is followed by recognition of the branch site by U2 snRNP, yielding splicing complex A. At the stage of dissociation of the 5′SS:U1 snRNA duplex and release of U1 snRNP, U4/U5/U6 tri-snRNP joins complex A to form splicing complex B, which subsequently rearranges into the catalytically active complex C. Several DExD/H-box proteins (ATPases/RNA helicases, or unwindases) identified both in yeast and mammalian systems are thought to mediate multiple RNA conformational changes occurring throughout the splicing process (reviewed in Staley & Guthrie, 1998; Murray & Jarrell, 1999). One of these factors, yPrp28p, has been implicated in the switch between the initial 5′SS:U1 snRNA duplex and the subsequent 5′SS:U6 snRNA pairing (Staley & Guthrie, 1998, 1999). However, a number of questions concerning the mechanism of action, recognition of RNA substrates, and interactions of these putative RNA helicases with other spliceosomal proteins remain to be answered.

Gorbalenya and Koonin (1993) classified helicases into three major superfamilies based on characteristic motifs shared by these proteins. Crystal structures of two DNA helicases; PcrA and Rep (Subramanya et al., 1996; Korolev et al., 1997; Velankar et al., 1999), and two RNA helicases; HCV NS3 and eIF4A (Yao et al., 1997; Kim et al., 1998), demonstrate that the conserved motifs required for ATP binding and hydrolysis are located at similar positions along the cleft separating two structurally similar protein domains. Helicases are known to be involved in several biological processes, including replication, translation, transcription, and pre-mRNA splicing (Schmid & Linder, 1992; Lüking et al., 1998). Among the DExD/H-box proteins involved in splicing, several exhibit single-stranded RNA-dependent ATPase activity in vitro (Schwer & Guthrie, 1991; Kim & Lin, 1996; O'Day et al., 1996; Raghunathan & Guthrie, 1998; Schwer & Gross, 1998; Wagner et al., 1998), but only in a few cases has the ATP-dependent RNA unwinding been demonstrated in vitro (Laggerbauer et al., 1998; Schwer & Gross, 1998; Wagner et al., 1998; Wang et al., 1998). Several human DExD/H-box proteins involved in splicing have been identified, including U5-200 kDa (Lauber et al., 1996), UAP 56 (Fleckner et al., 1997), hPrp16p (Zhou & Reed, 1998), hPrp28p (Teigelkamp et al., 1997), and HRH1 (Ono et al., 1994), which represent orthologs of yeast

Reprint requests to: Maria M. Konarska, The Rockefeller University, 1230 York Avenue, New York, New York 10021, USA; e-mail: konarsk@rockvax.rockefeller.edu.

Brr2p/Snu246/Prp44p, Sub2p, Prp16p, Prp28p, and Prp22p, respectively. In contrast to their yeast counterparts, hPrp28p and HRH1 proteins contain RS domains, and hPrp16p contains an N-terminal region rich in R, E, D, and S amino acids. However, the significance of the presence of these domains is not currently understood.

To analyze the complex structure and function of the spliceosome, a simplified in vitro system was developed, in which a short 5′SS RNA together with a longer 3′SS RNA are used as substrates in a bimolecular reaction (Konforti & Konarska, 1995). In this system, binding of the 5′SS to U1 snRNP is uncoupled from its subsequent interaction with U4/U5/U6 and U2 snRNPs, leading to formation of a homogeneous pool of complex B suitable for biochemical studies (Konforti et al., 1993). Furthermore, the 5′SS RNA can be easily modified, generating a specific probe to analyze biochemical processes associated with 5′SS recognition at the catalytic center and protein factors involved in this process. We have previously developed a two-step chemical modification strategy to incorporate photoreactive adducts at defined positions in the 5′SS RNA (Sha et al., 1998; Konarska, 1999). In the present study, we analyzed crosslinking profiles of the 5′SS RNA containing a benzophenone (BP) group at selected positions within the intron and detected a spliceosomal protein that interacts with the 5′SS at intron position +7/+8 within U2/U4/U5/U6 and U4/U5/U6 snRNP complexes. This protein, identified as the DEAD-box protein hPrp28p, interacts with the 5′SS in an ATP-dependent manner. The 5′SS:hPrp28p crosslink takes place already at the stage of complex B formation and is maintained throughout the splicing reaction. Furthermore, the 5′SS:hPrp28p contact correlates with the 5′SS:U6 snRNA interaction at the same intron positions (+7/+8). We have mapped the site of the 5′SS:hPrp28p crosslink to a short segment within the helicase domain of the protein (positions 601–609), spanning the highly conserved TAT motif that forms a part of the ATP-binding domain in hPrp28p. These findings strongly suggest that the 5′SS represents the functional substrate of hPrp28p, consistent with the proposed yPrp28p function in promoting the switch of the U1:5′SS to U6:5′SS pairing interactions. However, the 5′SS:hPrp28p contact does not require the initial 5′SS:U1 snRNA pairing, because the 5′SS:hPrp28p crosslink forms in the ATP-dependent fashion even in *trans*-splicing reactions in which the 5′SS is not allowed to base pair with U1 snRNA.

RESULTS

Probing the spliceosome with site-specifically derivatized 5′SS RNA

To characterize spliceosomal proteins in proximity of the 5′SS, we have used a previously described two-step chemical modification procedure (Sha et al., 1998) to site-specifically couple a photoreactive BP group at internal positions within the RNA substrate. The 11-nt 5′SS RNA used in the first series of experiments (Fig. 1A) contains a phosphorothioate residue at a specified position and carries in addition an adjacent 2′-

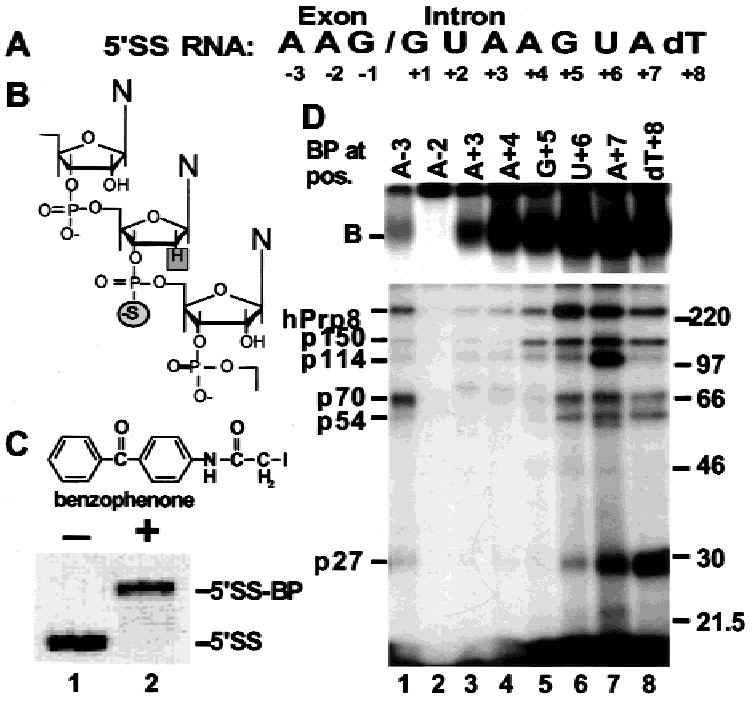

FIGURE 1. Under splicing conditions, the BP-derivatized 5′SS RNA crosslinks to a set of protein factors within complex B. **A**: The 11-nt 5′SS RNA contains a single phosphorothioate residue at the specified position. The position of modification refers to the phosphodiester bond at the 3′ side of the indicated nucleotide. The "/" indicates the exon/intron junction. **B**: Structure of a phosphorothioate RNA substrate used for derivatization reactions. The middle nucleotide in the shown fragment contains the phosphorothioate modification. **C**: Derivatization of the ^{32}P-thio-5′SS (lane 1) with BP-iodoacetamide couples the BP group to the sulfur in the 5′SS RNA, resulting in a decreased mobility of the product in a 20% polyacrylamide/8 M urea gel (lane 2). **D**: Splicing reactions using the labeled ^{32}P-5′SS RNA derivatized with BP at the indicated positions were incubated for 10 min at 30 °C, UV irradiated, and resolved in a 4% polyacrylamide native gel to monitor complex B formation. The gel segments containing complex B from individual reactions were excised and resolved in a second dimension in a 15% SDS gel. Positions of the 5′SS:protein crosslinks and the molecular weight markers are indicated.

deoxy group (Fig. 1B). Derivatization of this substrate with BP-iodoacetamide couples the BP group to sulfur in the 5′SS RNA, resulting in a decreased electrophoretic mobility of the product (Fig. 1C). Chemically synthesized 5′-end ^{32}P-labeled, BP-derivatized 5′SS RNA substrates, together with the 3′SS RNA containing the branch site, polypyrimidine tract, and the 3′ splice site, were used in bimolecular *trans*-splicing reactions in nuclear HeLa cell extracts (Konforti & Konarska, 1995). The reactions were irradiated with 302-nm UV light and the spliceosome complexes were resolved by nondenaturing gel electrophoresis. As previously observed for the APA-derivatized substrates (Sha et al., 1998), the bulky BP group positioned near the exon/intron junction (i.e., from positions -3 to $+3$) strongly interferes with complex B formation (Fig. 1D, lanes 1–3, and data not shown). The inhibitory effects of bulky groups in this region of the 5′SS RNA most likely reflect a steric hindrance with the hPrp8p:GU dinucleotide interaction (Reyes et al., 1996; Sha et al., 1998). This effect is not observed when BP is attached at more distal positions within the intron (positions $+4$ to $+8$), allowing for efficient complex B assembly (Fig. 1D, lanes 4–8). To detect spliceosomal components that contact the 5′SS through the BP group, UV-irradiated material present in complex B formed in individual reactions was first resolved in a nondenaturing gel and subsequently separated in an SDS-polyacrylamide gel (Fig. 1D). Under these conditions, the 5′SS RNA modified at intron positions $+7$ or $+8$ produces major crosslinks to p114 and p27 proteins (Fig. 1D, lanes 7 and 8). In addition, several minor crosslink products, including hPrp8p, p150, p70, and p54, can be detected in these reactions. The hPrp8p and p70 are crosslinked through thiol-nonspecific conjugation of BP occurring predominantly at adenosine residues in the 5′ exon of the 5′SS RNA (Konarska, 1999, and data not shown). The p150 can be detected only at early time points in the reaction (Fig. 2A).

The kinetics of crosslinking was compared between the *trans*- and *cis*-splicing systems (Fig. 2A). The 5′SS RNA used in these experiments contained a longer, 6-nt exon, and its two 3′-terminal nucleotides (dA$+7$ and dT$+8$) were introduced by enzymatic extension in the presence of a bridging DNA oligonucleotide, α-^{32}P-dATP, and thio-dTTP (Konarska, 1999). In parallel, the same 5′SS RNA was ligated to the 3′SS RNA to generate a full-length pre-mRNA substrate for *cis*-splicing (Moore & Sharp, 1992; Konarska, 1999). Both *trans*- and standard *cis*-splicing reactions yield similar results, producing the characteristic p114 crosslink (Fig. 2A), whose appearance coincides with formation of complex B (at 5 min for *trans*- and at 10 min for *cis*-splicing), and is maintained throughout splicing. Importantly, the 5′SS:p114 crosslink is still present at the time of splicing catalysis, as demonstrated by analysis of the RNA intermediates and products from similar *cis*- and *trans*-splicing reactions (Fig. 2B, and data not shown). This crosslinking profile is significantly different from that previously observed for the 5′SS:hPrp8p crosslink, which also appeared at the stage of complex B formation, but diminished at later stages in the reaction (Reyes et al., 1999). Moreover, the presence of the BP group can be detected not only in the input pre-mRNA substrate, but also in the lariat intermediates and products of splicing, as demonstrated by the characteristic decrease in gel mobility of RNase A-digested fragments of these RNAs (Fig. 2C). Thus, the BP group attached at intron position $+7$ does not interfere with either spliceosome formation (Fig. 1D, lane 7) or splicing catalysis monitored in either *cis*- or *trans*-splicing systems (Fig. 2B,C, and data not shown).

Consistent with its physical association with complex B (Fig. 1D), the 5′SS:p114 crosslink forms under conditions that allow for spliceosome assembly. Sequence-specific RNase H degradation of U2 or U6 snRNAs completely abolishes formation of the 5′SS:p114 crosslink in the *cis*-splicing system (Fig. 3A, lanes 1 and 2), whereas crosslink accumulation is unaffected by a mock treatment (Fig. 3A, lane 3). Interestingly, analogous disruption of snRNAs has different effects in the *trans*-splicing system, consistent with formation of the 5′SS-containing complexes under these conditions. Although degradation of U6 snRNA prevents formation of the 5′SS:p114 crosslink, a similar U2 snRNA disruption has no effect (Fig. 3A, lanes 4 and 5). In the *cis*-splicing system, both U2 and U6 snRNAs are required for stable association of the 5′SS with the spliceosome. In the functional *trans*-splicing reaction, however, the 5′SS can interact with U4/U5/U6 snRNP even in the absence of U2 snRNP, provided that the 5′ end of U1 snRNA is blocked or removed (Konforti & Konarska, 1994). Thus, the fact that under *trans*-splicing conditions, disruption of U2 snRNP does not affect the 5′SS:p114 crosslink indicates that the 5′SS:p114 contact can take place within U4/U5/U6 snRNP particle alone, and that U2 snRNP is not strictly required for this association. This conclusion is further supported by the presence of the 5′SS:U6 snRNA 254 nm UV crosslink generated in *trans*-splicing reactions, in which U2 snRNA has been destroyed (Fig. 3B, lane 2). Formation of this characteristic crosslink detected in mock-treated reactions is blocked by disruption of U6 snRNA, which prevents binding of the 5′SS to U4/U5/U6 snRNP (Fig. 3B, lanes 1 and 3).

Identification of p114 as the human ortholog of Prp28p

To identify p114, a large scale (300 μL) *trans*-splicing reaction using ^{32}P-labeled, BP-derivatized 5′SS RNA was incubated for 20 min at 30 °C, and subjected to 302 nm UV irradiation. The crosslinked products associated with spliceosomes were digested with RNase

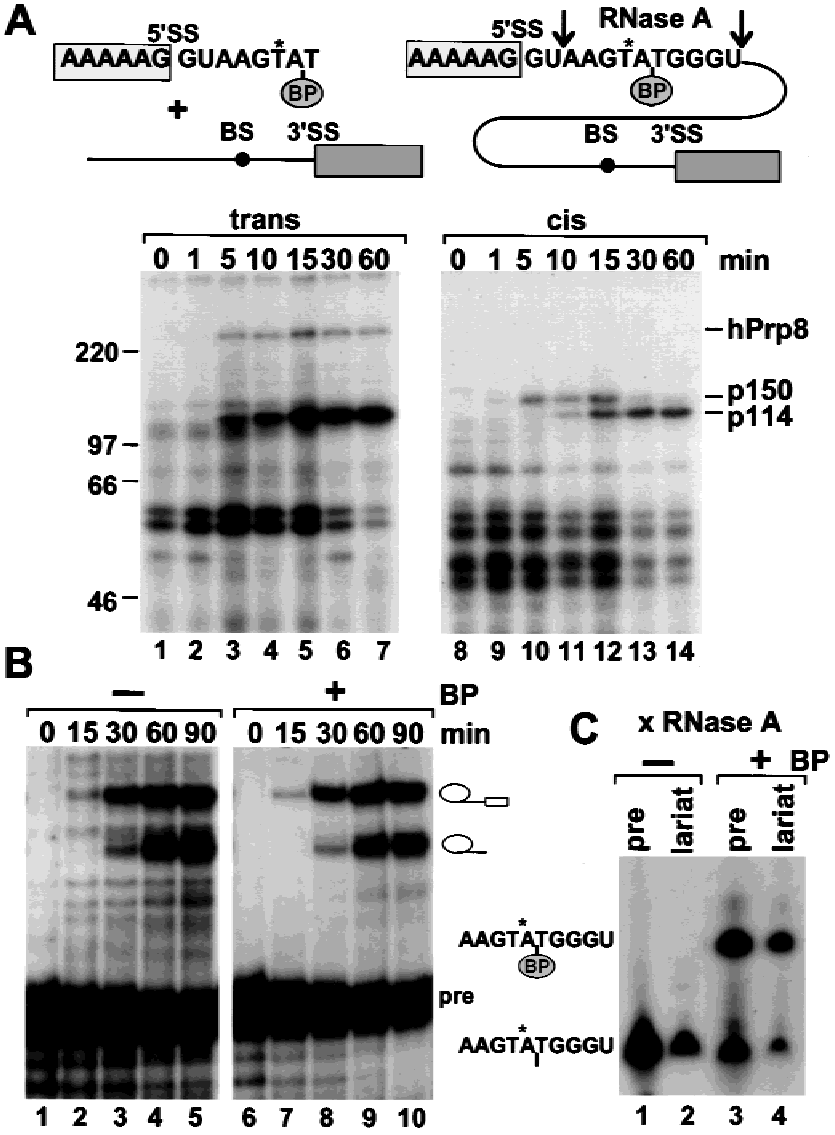

FIGURE 2. ^{32}P-labeled BP-derivatized substrates undergo splicing catalysis and crosslink to p114 protein in both *cis* and *trans*-splicing. **A**: The kinetics of crosslink of *trans*- and *cis*-splicing using ^{32}P-labeled BP-derivatized substrates. The crosslink appears at 5 min in *trans*-splicing (lane 3), and 10 min in *cis*-splicing (lane 11), and remains detectable throughout the splicing reactions. **B**: The BP group does not interfere with splicing catalysis. Splicing products were resolved in a 10% polyacrylamide/8 M urea gel. Kinetics (0 to 90 min) of splicing reactions using BP-derivatized *cis*-substrate indicates that splicing efficiency is comparable in the absence (lanes 1–5) or presence (lanes 6–10) of BP, as indicated by formation of lariat intermediates and products**. C**: Underivatized pre-mRNA (lane 1) and its lariat (lane 2) or derivatized pre-mRNA (lane 3) and its lariat (lane 4) were eluted from the denaturing gel (reactions shown in **B**) and treated with RNase A. The site of RNase A cleavage within the *cis*-substrate is indicated by the arrows in **A**.

T1, resolved by nonequilibrium pH gradient gel electrophoresis (NEPHGE) in the first dimension followed by SDS-PAGE in the second dimension, and transferred to a membrane for simultaneous detection of crosslinks and antibody reactivity. Positions of the labeled crosslink products (Fig. 4A) were visualized by autoradiography and compared to signals of the Western analysis (Fig. 4B) probed with antibodies against known spliceosomal proteins in the 100-kDa size range. The p114 crosslink detected by autoradiography migrates in close proximity of the U5 snRNP-100-kDa protein (Fig. 4C). In contrast, PSF, another splicing factor of a similar size (Patton et al., 1993), migrates as two spots with the isoelectric point more basic than that of U5-100-kDa protein (data not shown), consistent with earlier reports (Teigelkamp et al., 1997). The detectable shift between positions of the crosslink and endogenous U5-100-kDa protein signals can be explained by the presence of a 3-nt portion of the 5′SS RNA and the bulky, hydrophobic BP group, that remain attached to p114 crosslink after RNase T1 digestion. The 5′SS:p114 crosslink is immunoprecipitated with the specific anti-hPrp28p antibody (Fig. 4D, lane 2), identifying the crosslinked protein as the U5-100-kDa protein, termed here hPrp28p, the human ortholog of *Saccharomyces cerevisiae* splicing factor, yPrp28p (Teigelkamp et al., 1997).

Both yeast and human Prp28p proteins contain a C-terminal RNA helicase domain with a number of conserved motifs characteristic of the DEAD-box proteins, suggesting that they may be responsible for some RNA conformational rearrangements during splicing. In contrast to yPrp28p, hPrp28p contains an N-terminal RS domain characteristic of a family of SR protein splicing factors (Fu, 1995). Consistent with this feature, the 5′SS:p114 crosslink is immunoprecipitated with 16H3 (Fig. 4D, lane 3), a monoclonal antibody that recognizes RS domains independent of their phosphoryla-

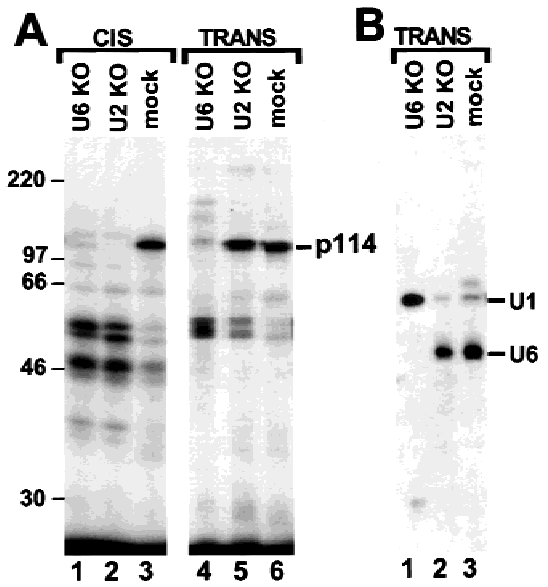

FIGURE 3. The 5′SS:p114 crosslink forms within U2/U4/U5/U6 snRNP complex in *cis*-splicing and does not require association of U2 snRNP in the *trans*-splicing system. **A**: SDS-PAGE analysis of *cis*- and *trans*-splicing reactions carried out with mock-treated (lanes 3 and 6) or RNase H-treated HeLa extracts in presence of oligonucleotides complementary to U2 (lanes 2 and 5) or U6 (lanes 1 and 4) snRNAs. Positions of the molecular weight markers are indicated. **B**: The 5′SS:snRNA crosslinks analyzed in a 13% polyacrylamide/8 M urea gel following *trans*-splicing reactions using RNase H-treated HeLa extracts, in the absence (lane 3) or presence of oligonucleotides complementary to U6 (lane 1) or U2 (lane 2) snRNAs. Note that although all reactions in **B** were carried out in the presence of the 5′SS DNA competitor, the 5′SS RNA still binds and crosslinks to low levels of the remaining free U1 snRNA in reactions, in which U6 snRNA is degraded (lane 1). Positions of the 5′SS:U1 and 5′SS:U6 snRNA crosslinks are indicated.

tion state (Neugebauer et al., 1995). Anti-PSF antibody was used as a negative control in this experiment (Fig. 4D, lane 4). Together, these results confirm that p114 represents hPrp28p, a 100-kDa component of U5 snRNP.

Formation of the 5′SS:hPrp28p crosslink correlates with NTP hydrolysis and the 5′SS:U6 snRNA base pairing interaction

To assess the NTP requirement of the 5′SS:hPrp28p interaction, *trans*-splicing reactions containing the BP-5′SS RNA were carried out in the presence of each of the four rNTPs, dATP, or nonhydrolyzable ATP analogs, and crosslink formation was monitored by SDS-PAGE (Fig. 5A). The 5′SS:hPrp28p crosslink forms efficiently in the presence of ATP and, in a comparable fashion, when UTP, CTP, GTP, or dATP, is used in the reaction (Fig. 5A, lanes 1–5). However, in the absence of ATP (Fig. 5A, lane 9), or in the presence of nonhydrolyzable ATP analogs (Fig. 5A, lanes 6 and 7), the 5′SS:hPrp28p crosslink is no longer detected. Instead, a distinct, faster migrating product, p112, becomes crosslinked to the 5′SS under these conditions. Immunoprecipitations carried out under denaturing conditions identify p112 as PSF (Fig. 5B), an essential splicing factor (Patton et al., 1993; Gozani et al., 1994). The 5′SS RNA:PSF crosslink forms only when the 5′ end of U1 snRNA is blocked or removed, indicating that the 5′SS paired to U1 snRNA is unable to interact with PSF (Fig. 5C).

In the presence of γ-S-ATP, which is hydrolyzed at a slower rate (if at all) as compared to ATP, the 5′SS:hPrp28p crosslink is detected at a strongly reduced level (Fig. 5A, lane 8). This suggests that not only the ATP presence, but rather its hydrolysis is required for the 5′SS:hPrp28p contact. In addition, *trans*-splicing reactions were carried out under conditions where the 5′ end of U1 snRNA was either removed or allowed to base pair with the 5′SS. Upon UV irradiation, crosslink products were analyzed in parallel by SDS-PAGE (Fig. 5C) and urea polyacrylamide (Fig. 5D) gels. Pairing of U1 snRNA to the 5′SS inhibits the 5′SS:hPrp28p crosslink, regardless of the presence or absence of ATP (Fig. 5C, lanes 1 and 2). Analysis of the RNA:RNA crosslinks indicates that only the 5′SS:U1, and not the 5′SS:U6 snRNA duplex, is detected under these conditions (Fig. 5D, lanes 1 and 2). In contrast, when U1 snRNA is prevented from pairing to the 5′SS, the 5′SS:hPrp28p crosslink forms efficiently, but only in the presence of ATP (Fig. 5C, lane 4), that is, under conditions that allow complex B assembly. Under these conditions, the 5′SS:U6 snRNA crosslink is also detected (Fig. 5D, lane 4). Thus, there is a perfect correlation between conditions required for spliceosome assembly, the 5′SS:U6 snRNA pairing interaction, and formation of the 5′SS:hPrp28p crosslink. Together, these results strongly suggest that the NTP-dependent 5′SS:hPrp28p crosslink and the 5′SS:U6 snRNA duplex are formed in the same complex.

Mapping of the 5′SS crosslink within hPrp28p

To identify the protein domain involved in contacting the 5′SS, the 5′SS:hPrp28p crosslink was subjected to proteolytic analysis, using both enzymatic (Glu-C and Arg-C) and chemical (CnBr, acetic acid) treatments (Reyes et al., 1999). By comparing the size of the cleavage fragments predicted from the known hPrp28p sequence with those generated by the enzymatic and chemical cleavage of the 5′SS:hPrp28p crosslink, it was possible to identify fragments that span the crosslink site. The 5′SS:hPrp28p crosslink was first digested with RNase T2 to reduce the portion of the 5′SS RNA attached to hPrp28p (Fig. 6A), SDS gel purified, and subjected to a series of enzymatic and chemical cleavages. Digestion products were resolved in parallel in a 22.5% SDS (Fig. 6B) and a 16% Tris-Tricine SDS gel (Fig. 6C) to allow for accurate size determination of the proteolytic fragments. The acid treatment results in the protein cleavage at Asp/Pro residues. Under denatur-

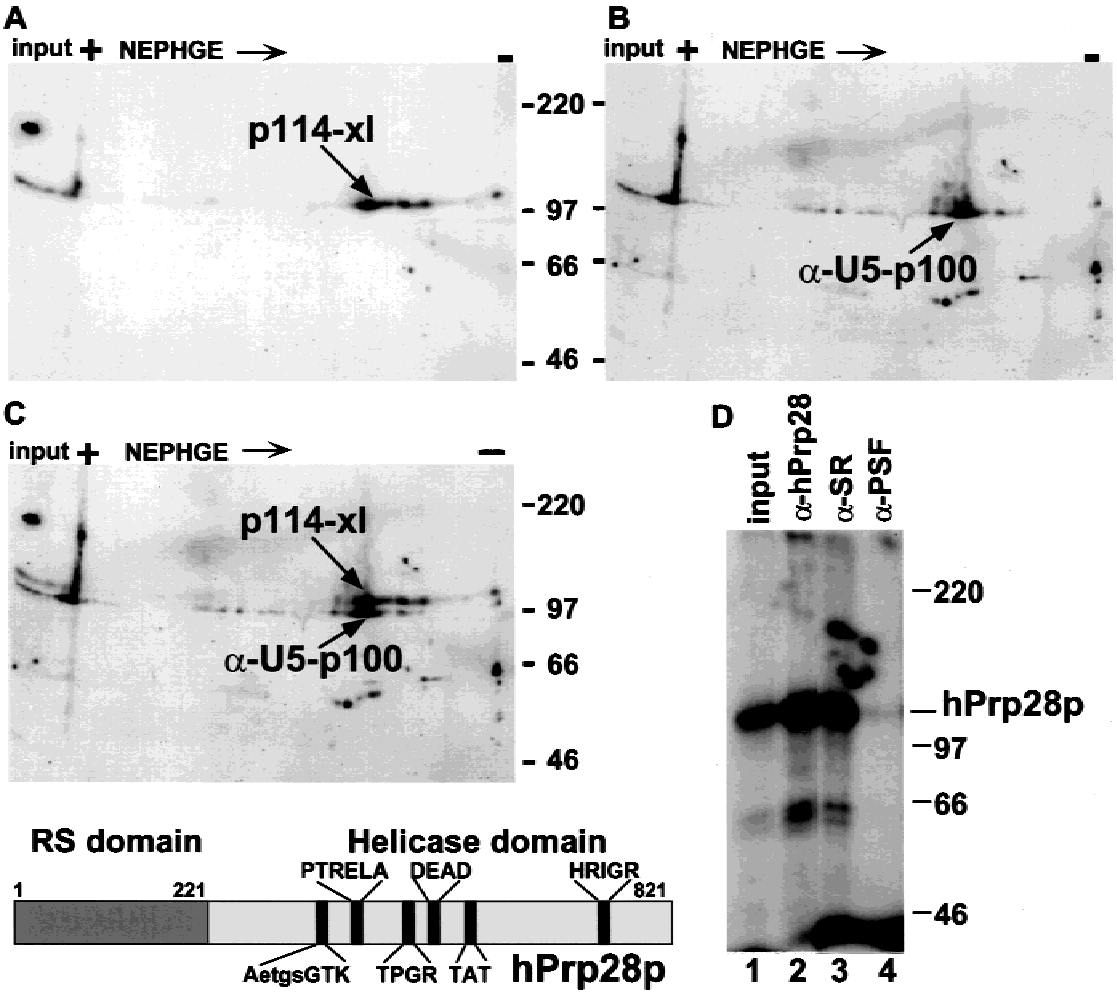

FIGURE 4. The p114 corresponds to hPrp28p (U5-p100K). **A**: A 300-μL splicing reaction using the ^{32}P-labeled BP-derivatized 5′SS RNA was UV irradiated for 3 min at 302 nm, spun through 900 μL of buffer D cushion, digested with RNase T1, and resolved in a NEPHGE (pH gradient from 4 to 10) in the first dimension and in a 8% SDS gel in the second dimension. The resolved material was electroblotted onto a nitrocellulose membrane and the position of the 5′SS:p114 crosslink (indicated by an arrow) was visualized by autoradiography. **B**: Western blot analysis with anti-U5-p100K (hPrp28p) antibody. Position of the U5-p100K is indicated by an arrow. **C**: Superimposition of **A** and **B** indicates that the p114 corresponds to U5-p100K protein (hPrp28p). **D**: Immunoprecipitation of crosslinking reactions was performed under denaturing conditions using anti-hPrp28p (lane 2), anti-SR (16H3) (lane 3), or anti-PSF antibodies (lane 4).

ing conditions the 5′SS:hPrp28p crosslink yields a single 9-kDa proteolytic fragment (Fig. 6B, lane 4). Because the hPrp28p sequence predicts the presence of just four acid cleavage fragments (44.2, 25.1, 17, and 9 kDa), the smallest of which corresponds to the 9 kDa peptide at positions 585–664, we conclude that the 5′SS crosslink is located within this fragment of hPrp28p. A 4.8-kDa crosslink-containing fragment is generated by Glu-C digestion (Fig. 6B, lane 1, and 6C, lane 2). Under the conditions used, Glu-C cleaves only after Glu, and not Asp residues (data not shown). Among the predicted Glu-C fragments located in proximity of positions 585–664, there are no peptides in the size range of 5 kDa. Instead, the observed 4.8-kDa fragment must represent a partial cleavage product spanning amino acid positions 594–637, in which the Glu-C cleavage site at position 614 is blocked (no cleavage between 2.3- and 2.5-kDa fragments). No other possible combinations of fragments consistent with the observed result can be found in this region of Prp28p. Similarly, the smallest product obtained from CnBr treatment (cleavage at the C-terminus of Met residues) is a 2.3-kDa fragment (Fig. 6B, lane 2) that corresponds to a partial digest spanning two fragments of 1.8 kDa (positions 589–604) and 0.5 kDa (positions 605–609). Even under more stringent CnBr cleavage conditions (37 °C, 16 h), the same 2.3-kDa fragment is observed (Fig. 6B, lane 5), indicating that in the context of the 5′SS:hPrp28p crosslink, the Met residue at position 609 is resistant to CnBr cleavage. The only other CnBr fragment that overlaps with the 9.2-kDa acid cleavage fragment is the 2-kDa peptide at positions 571–588; however, this pos-

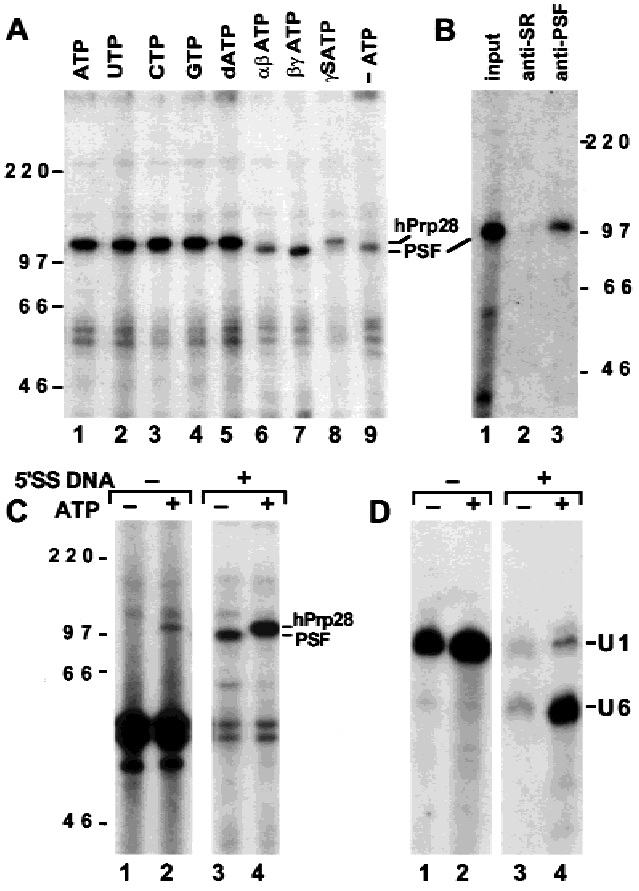

FIGURE 5. Formation of the 5′SS:hPrp28p crosslink requires NTP hydrolysis and correlates with the presence of the 5′SS:U6 snRNA duplex. **A**: *Trans*-splicing reactions were carried out in the presence of ATP, UTP, CTP, GTP, or dATP (lanes 1–5), in the absence of ATP (lane 9), or in the presence of ATP analogs AMP-CPP (α,β-ATP, lane 6), AMP-PNP (β,γ-ATP, lane 7), or γ-S ATP (lane 8). All NTPs (Sigma) were used at 1 mM concentration, in the absence of creatine phosphate in the reaction. Upon UV irradiation, the crosslink products were resolved in a 13% SDS gel. **B**: Immunoprecipitation of reactions carried out in the absence of ATP (lane 1) was performed under denaturing conditions using anti-SR (16H3, lane 2) or anti-PSF (lane 3) antibodies. **C**,**D**: Crosslinking reactions were conducted with extracts containing intact U1 snRNA (lanes 1 and 2) or with RNase H-treated extracts in the presence of DNA oligonucleotides complementary to the 5′ end of U1 snRNA, in the absence (lanes 1 and 3) or in the presence of ATP (lanes 2 and 4). The resulting 5′SS:hPrp28p and 5′SS:PSF crosslinks were analyzed in a 13% SDS gel (**C**), whereas the 5′SS:U1 and 5′SS:U6 snRNA crosslinks were resolved in a 10% polyacrylamide/8 M urea gel (**D**). Positions of the 5′SS:hPrp28p, 5′SS:PSF, 5′SS:U1, 5′SS:U6 snRNA crosslinks, and the molecular weight markers are indicated.

sibility is not consistent with the Glu-C digestion results. The fact that both CNBr and Glu-C treatments yield partial digestion products may reflect interference due to the BP crosslink in proximity of the cleavage sites. Digestion of the 5′SS:hPrp28p crosslink with Lys-C (cleavage after Lys residues) yields a single 4.0-kDa fragment (Fig. 6C, lane 1). In the hPrp28p sequence, there are two possible peptides of that size; one at positions 205–236, which is inconsistent with all the other results, and another at positions 599–634, located within the Glu-C 4.8-kDa partial fragment at positions 594–637 (Fig. 6B, lane 1, and 6C, lane 2). Furthermore, a double Glu-C plus Lys-C digest generates the same 4-kDa fragment, confirming that the Lys-C peptide containing the crosslink must be located within the 4.8-kDa Glu-C fragment, because the other Lys-C peptide contains multiple ER dipeptide repeats and would be digested with Glu-C. Finally, Arg-C digestion of the 5′SS:hPrp28p crosslink generates a single fragment of ~1.7 kDa (Fig. 6C, lane 3). Within the analyzed region of hPrp28p, there is only one predicted peptide in that size range, a 1.7-kDa fragment at positions 601–615. Taken together, the above results limit the location of the 5′SS:hPrp28p crosslink to a short, 9 amino acid fragment at positions 601–609. This segment (QTVMFTATM) spans the highly conserved TAT motif that forms a part of the ATP-binding site of the protein.

DISCUSSION

Numerous RNA rearrangements are required for spliceosome assembly and formation of its catalytic center. To better understand complex interactions leading to the proper positioning of the splice sites for catalysis, we have analyzed spliceosomal factors positioned in proximity of the benzophenone-derivatized 5′SS. The BP group coupled to the 5′SS RNA at positions +7 and +8 forms two major crosslinks to p27, an unidentified spliceosomal protein, and the 100-kDa component of U5 snRNP, a human ortholog of *S. cerevisiae* Prp28p splicing factor (Teigelkamp et al., 1997). The human Prp28p is a stable component of U5 snRNP and U4/U5/U6 snRNP particles. Both yeast and human Prp28p contain a highly conserved C-terminal RNA helicase domain with motifs characteristic of the DExD/H-box proteins (Teigelkamp et al., 1997). To date, no RNA helicase activity has been detected in vitro for either yeast or human Prp28p, suggesting that Prp28p either requires specific interactions provided by the U4/U5/U6 snRNP, or that in the purified form, it lacks some subunit(s) needed for activity. The yPrp28p is an essential factor required prior to the first catalytic step of splicing (Strauss & Guthrie, 1991, 1994), implicated in destabilization of the 5′SS:U1 snRNA pairing prior to formation of the 5′SS:U6 snRNA duplex (Staley & Guthrie, 1999). However, the detailed mechanism of yPrp28p function in splicing is not known.

In HeLa cell extracts, the 5′SS:hPrp28p crosslink forms at the stage of complex B assembly and remains detectable throughout the reaction, suggesting that the relative positions of hPrp28p and the 5′SS remain mostly unchanged during splicing. This is in sharp contrast to the crosslinking profile observed for the 5′SS:hPrp8p interaction at the 5′ splice site junction (Reyes et al., 1999), which was characterized only by a transient signal at the initial stages of complex B formation. The site of contact between the 5′SS and hPrp28p is located

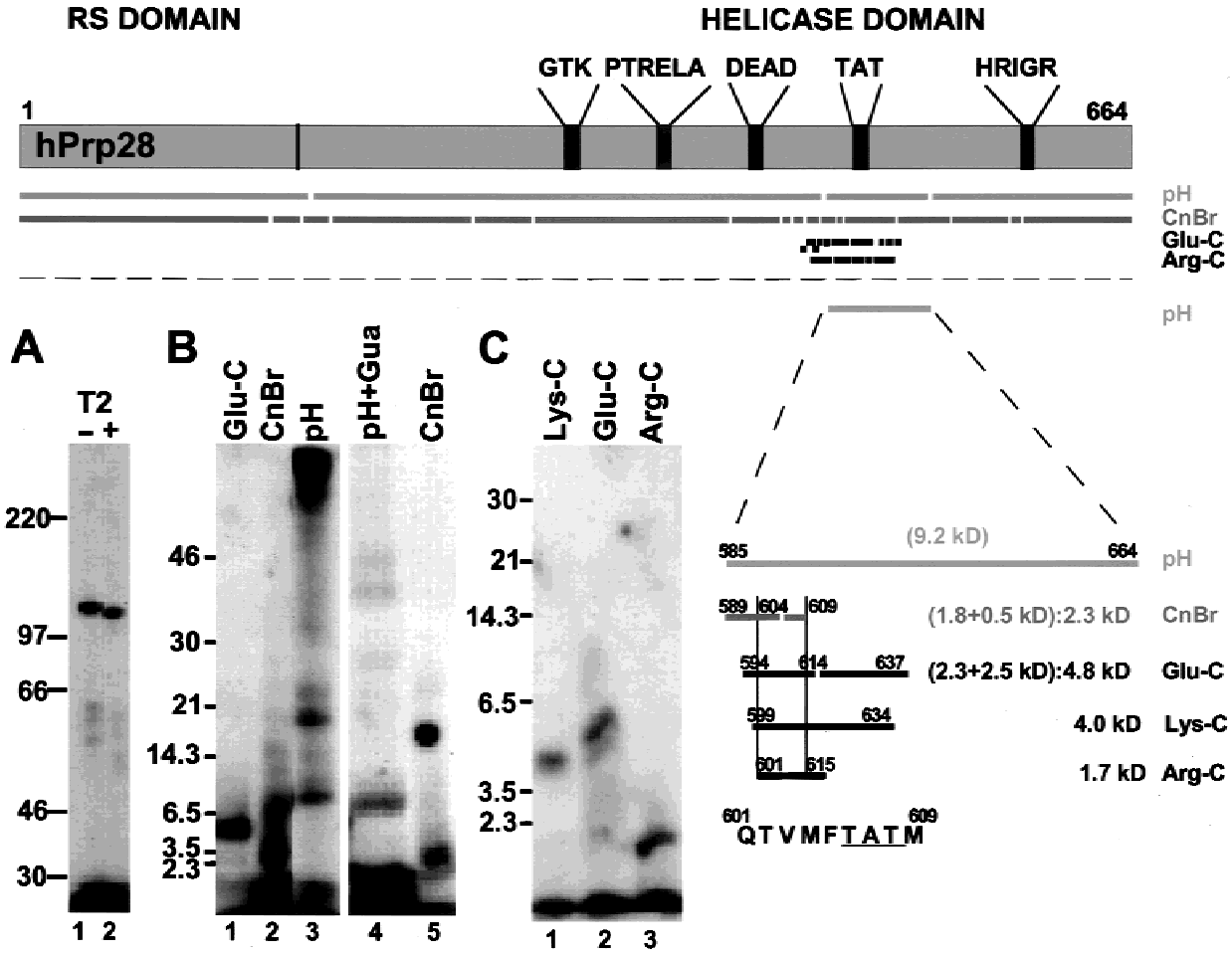

FIGURE 6. Mapping of the site of the 5′SS RNA crosslink within hPrp28p. **A**: A 300-μL crosslinking reaction using the ^{32}P-labeled BP-derivatized 5′SS RNA was spun through a 900 μL cushion of buffer D and the pellet was treated with RNase T2. Aliquots (5 μL) from the reaction, before (lane 1) and after RNase T2 treatment (lane 2), were resolved in a 13% polyacrylamide SDS gel to control for RNase T2 digestion. **B**: The 5′SS:hPrp28p crosslink was gel purified and digested with Glu-C (lane 1) protease, or treated with cyanogen bromide (CnBr) either at 25 °C (lane 2) or at 37 °C (lane 5). The acid treatment was carried out in the presence of 13% acetic acid (lane 3) or 13% acetic acid, 6 M guanidinium chloride (lane 4). Digestion products were resolved in a 22.5% SDS gel and visualized by autoradiography. **C**: Enzymatic digestions of the 5′SS:hPrp28p crosslink with Lys-C (lane 1), Glu-C (lane 2), and Arg-C (lane 3) proteases. Digestion products were resolved in a 16% Tris-Tricine gel. Positions of the molecular weight markers are indicated. The schematic summarizes the mapping analysis of the 5′SS:hPrp28p crosslink. Size and position of fragments predicted from hPrp28p sequence are shown for the acidic treatment (pH), cyanogen bromide (CnBr), Lys-C, Glu-C, and Arg-C proteases.

only a few nucleotides away from the 5′SS:hPrp8p interaction at the conserved GU dinucleotide (Reyes et al., 1996), suggesting that hPrp28p and hPrp8p must be positioned in a close proximity of each other within the U4/U5/U6 snRNP (Fig. 7). Indeed, a genetic interaction has been demonstrated between yeast Prp8p and Prp28p (Strauss & Guthrie, 1991). The 5′SS:hPrp28p crosslink is detectable both in *cis*- and *trans*-splicing systems. Because the main difference between these in vitro systems concerns the initial 5′SS:U1 snRNA pairing, which is required for *cis*-splicing but bypassed in *trans*-splicing reactions, we conclude that the 5′SS:hPrp28p interaction does not strictly depend on this step in spliceosome assembly. Although the integrity of U6 snRNA is essential for the 5′SS:hPrp28p crosslink in both *trans*- and *cis*-splicing reactions, intact U2 snRNA is required only under *cis*-splicing conditions (Fig. 3), suggesting that the 5′SS:hPrp28p contact occurs already within U4/U5/U6 snRNP and does not strictly require U2 snRNP. Similarly, in *trans*-splicing reactions, formation of the 5′SS:U6 snRNA duplex requires intact U6, but not U2 snRNA (Konforti & Konarska, 1994; Fig. 3). Positions within the 5′SS RNA that support crosslinking to hPrp28p (peak at positions +7) fall within the region involved in the 5′SS:U6 snRNA pairing interaction (positions 40–42 in hU6 snRNA; Wassarman & Steitz, 1992), suggesting that hPrp28p contacts not the 5′SS alone, but rather the 5′SS:U6

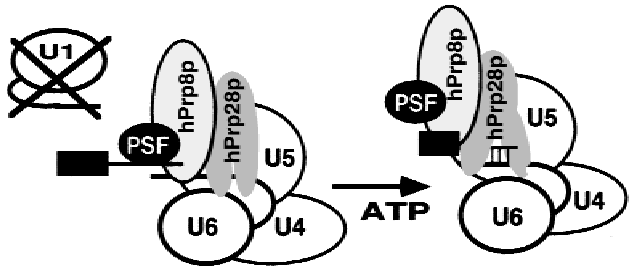

FIGURE 7. Proposed scheme for interactions between the 5′SS and the spliceosomal components leading to the stable 5′SS:U4/U5/U6 snRNP association. Under conditions when the 5′SS is prevented from base-pairing with U1 snRNA, and in the absence of ATP, the 5′SS interacts with PSF, most likely in a semistable association with U4/U5/U6 snRNP. Upon hPrp28p-mediated ATP binding and hydrolysis, the 5′SS is translocated into the complex, resulting in a base-pairing interaction with U6 snRNA. At this stage the 5′SS junction is known to interact with hPrp8p. The relative positions of the components are arbitrary. See text for further details.

snRNA duplex. This 5′SS:U6 snRNA:hPrp28p contact is established already at the stage of the 5′SS:U4/U5/U6 snRNP association, and may persist throughout the splicing reaction.

Location of the 5′SS RNA crosslink within hPrp28p

Important information concerning the 5′SS:hPrp28p interaction was obtained from the mapping of the site of crosslink within the protein. Because of the remarkable specificity of the BP-mediated crosslinking, the resulting product is virtually homogenous, representing a single contact between the 5′SS RNA and hPrp28p. The crosslink site maps to a short segment in the helicase domain of hPrp28p (amino acid positions 601–609), spanning the conserved TAT motif (motif III, positions 606–608; Lüking et al., 1998). Mutational studies suggested that motif III (which in many other DExD/H-box proteins contains an SAT rather than TAT sequence) is involved in coupling ATP hydrolysis with duplex unwinding (Schwer & Guthrie, 1992; Plumpton et al., 1994; Gross & Shuman, 1998). In fact, in several DExH-box proteins, mutations of this motif result in inhibition of splicing (Plumpton et al., 1994; B. Schwer, pers. comm.). Based on the structural similarity of several helicases, including PcrA and Rep DNA helicases (Subramanya et al., 1996; Korolev et al., 1997) and HCV RNA helicase (Yao et al., 1997), a unifying mechanism for this class of proteins has been suggested (Bird et al., 1998). Helicases coordinate a cycle of ATP binding and hydrolysis to an ordered series of conformational changes that allow the protein to move along its substrate. Because of its localization in a hinge region connecting the two protein domains, motif III is thought to play a pivotal role in these conformational changes. The current models predict that, upon binding of ATP and the single stranded portion of the substrate, the protein assumes a closed conformation. Subsequent ATP hydrolysis yields an opened conformation of the protein, resulting in a stretched motion that pulls the single strand of RNA (or DNA) and as a result, unwinds the substrate duplex. The structural organization of helicases requires that during catalysis, the single-stranded substrate is positioned in proximity of the conserved motif III hinge connecting the two protein domains that undergo the ATP-dependent conformational changes (Bird et al., 1998; Velankar et al., 1999). Although the structure of hPrp28p is not currently known, its TAT motif most likely also connects the two conformationally changing domains of the protein. If the position of the single-stranded RNA relative to motif III is similar in hPrp28p and HCV NS3 RNA helicase, the observed BP-mediated crosslink (~15 Å linker) between the 5′SS RNA and the TAT motif of hPrp28p is fully consistent with the predicted structure, strongly suggesting that the 5′SS represents a true substrate for hPrp28p. Although it is formally possible that the observed 5′SS:hPrp28p crosslink reflects only a close proximity, and not the direct contact between the 5′SS and the helicase, the simplest interpretation is that the crosslink results from the proper positioning of the 5′SS in the opened conformation of hPrp28p. In fact, the present study offers the first biochemical evidence of the direct, specific contact between an RNA substrate and its putative RNA helicase.

Correlation between NTP hydrolysis and the 5′SS:hPrp28p interaction

Formation of the 5′SS:hPrp28p crosslink requires the presence of a hydrolyzable form of NTP. In its absence, formation of the 5′SS:hPrp28p crosslink is strongly inhibited and a distinct 5′SS:PSF crosslink is generated instead (Fig. 5). PSF, an essential splicing factor, can be detected in purified U4/U5/U6 snRNP particles (Teigelkamp et al., 1997) and in splicing complex B, but it is strongly enriched in complex C (Gozani et al., 1994). These findings implicate PSF in the second catalytic step; however, earlier studies suggested that it may function already prior to complex A formation (Patton et al., 1993). The 5′SS:PSF crosslink is detectable only when the 5′ end of U1 snRNA is blocked and only in the absence of NTP hydrolysis (Fig. 5), suggesting that PSF contacts the 5′SS prior to formation of the first ATP-dependent complexes, but possibly after destabilization of the 5′SS:U1 snRNA pairing. It is likely that PSF contacts the 5′SS in an NTP-independent, semistable association with U4/U5/U6 snRNP that does not involve the 5′SS:U6 snRNA pairing (S. Kameoka and M. Konarska, in prep.).

In contrast to the NTP-independent 5′SS:PSF association, NTP hydrolysis appears to be required for the

5′SS:U6 snRNA:hPrp28p interaction. Because hPrp28p belongs to the DEAD-box family of putative helicases, the 5′SS:hPrp28p crosslink requires the presence of NTP, and maps to the conserved motif III expected to lie in proximity of the RNA pulled into the protein in the NTP-dependent fashion; the simplest interpretation is that the 5′SS:hPrp28p contact results directly from hPrp28p-mediated NTP and RNA binding (Fig. 7). It is tempting to speculate that this reaction constitutes the ATP-dependent step observed at the stage of the 5′SS:U4/U5/U6 snRNP interaction (Konforti & Konarska, 1994; Maroney et al., 2000). At the moment, no other NTP-dependent steps are known to operate at this stage of splicing, although their existence cannot be excluded. It is possible that in addition to hPrp28p, other DExD/H-box spliceosomal proteins are involved. One possible candidate is the U5-200-kDa protein, a human ortholog of *S. cerevisiae* Brr2p/Snu246p/Prp44p, that exhibits an ATPase/RNA helicase activity in vitro (Lauber et al., 1996; Kim & Rossi, 1999). The ATPase/RNA helicase activities required for complex A formation are unlikely to be involved here, as U2 snRNP is not required for association of the 5′SS with U4/U5/U6 snRNP and the 5′SS:hPrp28p interaction.

Implications for the positioning of the 5′ splice site within the spliceosome

The switch of the early 5′SS:U1 snRNA pairing for the 5′SS:U6 snRNA interaction is critical for the proper recognition and positioning of the 5′SS within the spliceosome. A combination of genetic and biochemical analyses identified yPrp28p as the likely catalyst of this ATP-dependent RNA rearrangement (Staley & Guthrie, 1999). Out of a large collection of mutant splicing factors that included a number of other ATPases of the DExD/H-box family, only prp28-1 exacerbated the cold-sensitive defect caused by hyperstabilization of the 5′SS:U1 snRNA pairing. Furthermore, the 5′SS:U1 snRNA intermediates could be chased into functional spliceosomes in vitro in the presence of ATP and yPrp28p (Staley & Guthrie, 1999), suggesting that yPrp28p itself unwinds the 5′SS:U1 snRNA duplex, allowing for the subsequent 5′SS:U6 snRNA pairing. However, the detailed mechanism by which this strand exchange between U1 and U6 snRNAs is achieved is not understood.

In the HeLa cell system, formation of the 5′SS:hPrp28p crosslink is detected not only in standard *cis*-splicing reactions, but also under *trans*-splicing conditions, that is, when U1 snRNA is not allowed to base pair with the 5′SS. Formation of the 5′SS:hPrp28p crosslink requires NTP hydrolysis in both *cis*- and *trans*-splicing reactions, suggesting that the absence of the 5′SS:U1 snRNA pairing is not sufficient for the subsequent hPrp28p-dependent association of the 5′SS with U6 snRNA. In fact, the two reactions involved in this strand exchange, that is, unwinding of the 5′SS:U1 snRNA and formation of the 5′SS:U6 snRNA duplex, do not necessarily need to be independent of each other. It is possible to view the unwinding of the 5′SS:U1 snRNA duplex by hPrp28p as a simple consequence of the NTP-dependent conformational change in the protein, that, at the same time, positions the unwound 5′SS in proximity of U6 snRNA, promoting formation of a new duplex. According to this view, hPrp28p unwindase acts also as a 5′SS translocase that requires NTP hydrolysis to properly position the 5′SS within the spliceosome, regardless of whether the 5′SS is originally duplexed with U1 snRNA. It is possible that other DExD/H-box proteins involved in splicing act in a similar way, executing ATP-dependent translocations of RNA segments, in some cases causing their unwinding, but always changing their position within the complex.

It is not clear to what extent the interactions between Prp28p, the 5′SS, and U6 snRNA detected in HeLa cell extracts are paralleled in the yeast system. Unlike the HeLa protein, Prp28p in yeast is not stably associated with U5 or U4/U5/U6 snRNPs (Gottschalk et al., 1999), and its interaction with U6 snRNA has not been detected (Vidal et al., 1999). Furthermore, the 5′SS:U1 snRNA pairing appears to be indispensable for splicing in yeast, whereas under appropriate conditions it can be bypassed in mammalian systems (Crispino et al., 1994; Tarn & Steitz, 1994; Konforti & Konarska, 1995). Thus, it is possible that the mechanisms responsible for the 5′SS:U1 to 5′SS:U6 snRNA switch may show some differences between the two systems. In fact, in *S. cerevisiae*, the requirement for Prp28p can be bypassed in strains carrying mutated forms of either U1C protein or U1 snRNA, in which the 5′SS:U1 snRNA duplex is destabilized (T.-H. Chang, pers. comm.). The yPrp28p requirement is restored in the presence of a mutant yPrp8p, suggesting that all these factors act together at the stage of the 5′SS:U1 to 5′SS:U6 snRNA switch. Our analysis demonstrates that the 5′SS contacts at least three spliceosomal proteins; hPrp8p at the splice junction (Reyes et al., 1996), and hPrp28p and p27 at intron positions $+7$ and $+8$ (Fig. 1), all of which are likely to contribute to proper positioning of the 5′SS within the complex. Also, genetic analysis in yeast indicates that the 5′SS:Prp8p interaction at the splice junction is important for splicing catalysis (Collins & Guthrie, 1999; Siatecka et al., 1999). It is possible that the 5′SS is held in place for catalysis even in the absence of Prp28p interacting with the 5′SS:U6 snRNA duplex, perhaps with some loss in fidelity of the 5′SS recognition, provided that the proper contacts between Prp8p and the 5′ splice junction are maintained. Although further studies are necessary to clarify these issues, the overall striking conservation of splicing mechanisms strongly suggests that at least some of the interactions described here for HeLa cells function also in other systems.

MATERIALS AND METHODS

RNA substrates

The RNA substrates were as described (Sha et al., 1998; Konarska, 1999). The 5′SS RNA used in Figure 1 contained the thiol and 2′H groups at specified positions. In all other experiments, a 5′AAAAAG/GUAAGdT^{32}P-dA-thio-dT3′ RNA oligonucleotide was used. Preparation of this substrate and its derivatization with benzophenone 4-iodoacetamide (Molecular Probes) was as described (Konarska, 1999). The extent of derivatization was monitored in a 20% polyacrylamide/8 M urea gel (Fig. 1C).

The 3′SS RNA used in *trans*-splicing experiments contained a 83-nt intron and 45-nt exon transcribed from pBSAd13 plasmid (Konarska, 1989). For *cis*-splicing reactions, this RNA was ligated to the ^{32}P-labeled, BP-derivatized 5′SS RNA described above to generate a full-length pre-mRNA substrate (Moore & Sharp, 1992; Konarska, 1999).

UV crosslinking

Preparation of HeLa cell nuclear extracts and *trans*-splicing reactions was as described (Konforti & Konarska, 1995). Splicing reactions were transferred to a microtiter plate embedded in ice and UV irradiated at 254 nm 3 × 4 min for RNA–RNA crosslinks, or at 302 nm for 3 min for RNA–protein crosslinks detection. To reduce the background of nonspliceosomal crosslinks, reactions (10 μL) were spun through a 100-μL cushion of buffer D (20 mM HEPES, pH 7.6, 20% glycerol, 100 mM KCl, 0.2 mM EDTA) at 4 °C for 20 min at 70k rpm in a Beckman TL-100 ultracentrifuge in a TLA 100.3 rotor and resolved by SDS-PAGE. To analyze RNA–RNA crosslinks, samples were proteinase K treated, phenol extracted, and resolved in a 10% acrylamide/8 M urea gel.

In addition, the 5′SS DNA, 5′CAGGTAAGTAT3′, and DNA oligonucleotides complementary to the following regions of human snRNAs were used: U1: 1–11, U2g: 29–42, and U6f: 33–48.

NTP requirement analysis

HeLa NE (60 μL) was incubated in a 77-μL knock-out reaction in the presence of 10 μg of the 5′SS DNA oligonucleotide (complementary to the nt 1–11 of U1 snRNA), 1.5 mM $MgCl_2$, and 4 U of RNase H (Boehringer). The reaction was incubated for 10 min at 37 °C, followed by 50 min at 30 °C. Subsequent *trans*-splicing assays (10 μL) contained 5 μL of the above U1 knock-out reaction, and were supplemented with the indicated NTPs (1 mM) and $MgCl_2$ (2 mM final concentration). No creatine phosphate was used in these experiments. Reactions were UV irradiated and analyzed as described above.

Immunoprecipitation under denaturing conditions

Trans-splicing reactions (100 μL) were conducted using ^{32}P-labeled (5 × 10^6 cpm), BP-derivatized 5′SS RNA. Upon UV crosslinking, the products were spun through a buffer D cushion, and resuspended in 100 μL IP-100 (100 mM NaCl, 50 mM Tris, pH 7.5, 2 mM $MgCl_2$, 0.5 mM DTT) containing 1% empigen (CalBiochem) and 1 μg RNase A. Following a 10-min incubation at 25 °C, samples were mixed with Protein A-Trisacryl beads (PIERCE) prebound to specific antibodies, rocked at 4 °C for 2 h, washed twice with 200 μL IP-100, 0.05% NP40, and once with IP-150 (150 mM NaCl, 50 mM Tris, pH 7.5, 2 mM $MgCl_2$ 0.5 mM DTT, 0.05% NP40, 1 M urea).

Mapping of the crosslink site within the protein

Trans-splicing reactions (300 μL) were UV irradiated at 302 nm for 3 min and centrifuged through a 900-μL cushion of buffer D for 30 min at 70k rpm. The pellet was treated with RNase T1 (3 μg) for 30 min at 37 °C and the 5′SS:hPrp28p crosslink was gel purified from an 11% polyacrylamide SDS gel. The precipitated material (typically ~1 kcpm) was digested with endoproteases Glu-C (2 U) in 0.2 M ammonium bicarbonate, pH 7.8, Arg-C (2 U) in sodium acetate, pH 7.4, for 2 h at 37 °C, or Lys-C (2 U) in 0.1 M ammonium bicarbonate, pH 8.5, for 11 h at 37 °C. Reactions were stopped by adding 1 vol of 2× SDS loading buffer. CnBr was adjusted to 40 mg/mL with 70% formic acid in 50 μL and the reaction was incubated overnight either at room temperature (Fig. 6B, lane 2), or at 37 °C (Fig. 6B, lane 5). The acid cleavage (100 μL) was carried out in 13% acetic acid (Fig. 6B, lane 3) or 13% acetic acid/6 M guanidium chloride (Fig. 6B, lane 4) at 37 °C for 6 h. CnBr and acid-treated samples were ethanol precipitated in the presence of 10 mM Tris-base. Digestion products were resolved in parallel in Laemmli 22.5% polyacrylamide/SDS and 16% polyacrylamide/6 M urea Tris-Tricine SDS gels (Schägger & von Jagow, 1987).

ACKNOWLEDGMENTS

We thank Drs. Bernhard Laggerbauer and Reinhard Lührmann, IMT Marburg, and Jim Patton, Vanderbilt University, Nashville, Tennessee, for their generous gifts of anti-U5-100K and anti-PSF antibodies, respectively. We also thank Charles Query and Beate Schwer for critical reading of the manuscript. N.I. and M.S. were supported by Norman and Rosita Winston Postdoctoral Fellowships. This work was supported by National Institutes of Health grant GM 49044 to M.M.K.

Received September 5, 2000; returned for revision October 5, 2000; revised manuscript received October 30, 2000

REFERENCES

Bird LE, Subramanya HS, Wigley DB. 1998. Helicases: A unifying structural theme? *Curr Opin Struct Biol 8*:14–18.

Collins CA, Guthrie C. 1999. Allele-specific genetic interactions between Prp8 and RNA active site residues suggest a function for Prp8 at the catalytic core of the spliceosome. *Genes & Dev 13*:1970–1982.

Crispino JD, Blencowe BJ, Sharp PA. 1994. Complementation by SR proteins of pre-mRNA splicing reactions depleted of U1 snRNP. *Science 265*:1866–1869.

Fleckner J, Zhang M, Valcarcel J, Green MR. 1997. U2AF65 recruits a novel human DEAD box protein required for the U2 snRNP-branchpoint interaction. *Genes & Dev 11*:1864–1872.

Fu XD. 1995. The superfamily of arginine/serine-rich splicing factors. *RNA 1*:663–680.

Gorbalenya AE, Koonin EV. 1993. Helicases: Amino acid sequence comparisons and structure–function relationships. *Curr Opin Struc Biol 3*:419–429.

Gottschalk A, Neubauer G, Banroques J, Mann M, Lührmann R, Fabrizio P. 1999. Identification by mass spectrometry and functional analysis of novel proteins of the yeast [U4/U6.U5] tri-snRNP. *EMBO J 18*:4535–4548.

Gozani O, Patton JG, Reed R. 1994. A novel set of spliceosome-associated proteins and the essential splicing factor PSF bind stably to pre-mRNA prior to catalytic step II of the splicing reaction. *EMBO J 13*:3356–3367.

Gross CH, Shuman S. 1998. The nucleoside triphosphatase and helicase activities of vaccinia virus NPH-II are essential for virus replication. *J Virol 72*:4729–4736.

Kim DH, Rossi JJ. 1999. The first ATPase domain of the yeast 246-kDa protein is required for in vivo unwinding of the U4/U6 duplex. *RNA 5*:959–971.

Kim JL, Morgenstern KA, Griffith JP, Dwyer MD, Thomson JA, Murcko MA, Lin C, Caron PR. 1998. Hepatitis C virus NS3 RNA helicase domain with a bound oligonucleotide: The crystal structure provides insights into the mode of unwinding. *Structure 6*:89–100.

Kim SH, Lin RJ. 1996. Spliceosome activation by PRP2 ATPase prior to the first transesterification reaction of pre-mRNA splicing. *Mol Cell Biol 16*:6810–6819.

Konarska MM. 1989. Analysis of splicing complexes and small nuclear ribonucleoprotein particles by native gel electrophoresis. *Methods Enzymol 180*:442–453.

Konarska MM. 1999. Site-specific derivatization of RNA with photocrosslinkable groups. *Methods 18*:22–28.

Konforti BB, Konarska MM. 1994. U4/U5/U6 snRNP recognizes the 5′ splice site in the absence of U2 snRNP. *Genes & Dev 8*:1962–1973.

Konforti BB, Konarska MM. 1995. A short 5′ splice site RNA oligo can participate in both steps of splicing in mammalian extracts. *RNA 1*:815–827.

Konforti BB, Koziolkiewicz MJ, Konarska MM. 1993. Disruption of base pairing between the 5′ splice site and the 5′ end of U1 snRNA is required for spliceosome assembly. *Cell 75*:863–873.

Korolev S, Hsieh J, Gauss GH, Lohman TM, Waksman G. 1997. Major domain swiveling revealed by the crystal structures of complexes of *E. coli* Rep helicase bound to single-stranded DNA and ADP. *Cell 90*:635–647.

Laggerbauer B, Achsel T, Lührmann R. 1998. The human U5-200 kD DEXH-box protein unwinds U4/U6 RNA duplices in vitro. *Proc Natl Acad Sci USA 95*:4188–4192.

Lauber J, Fabrizio P, Teigelkamp S, Lane WS, Hartmann E, Lührmann R. 1996. The HeLa 200 kDa U5 snRNP-specific protein and its homologue in *S. cerevisiae* are members of the DEXH-box protein family of putative RNA helicases. *EMBO J 15*:4001–4015.

Lüking A, Stahl U, Schmidt U. 1998. The protein family of RNA helicases. *Crit Rev Biochem Mol Biol 33*:259–296.

Maroney PA, Romfo CM, Nilsen TW. 2000. Functional recognition of the 5′ splice site by U4/U6.U5 tri-snRNP defines a novel ATP-dependent step in early spliceosome assembly. *Mol Cell 6*:317–328.

Moore MJ, Query CC, Sharp PA. 1993. Splicing of precursors to mRNA by the spliceosome. In: Gesteland RF, Atkins JF, eds., *The RNA world*, Cold Spring Harbor, New York: Cold Spring Harbor Laboratory Press. pp 303–357.

Moore MJ, Sharp PA. 1992. Site-specific modification of pre-mRNA: The 2′-hydroxyl groups at the splice sites. *Science 256*:992–997.

Murray HL, Jarrell KA. 1999. Flipping the switch to an active spliceosome. *Cell 96*:599–602.

Neugebauer KM, Stolk JA, Roth MB. 1995. A conserved epitope on a subset of SR proteins defines a larger family of pre-mRNA splicing factors. *J Cell Biol 129*:899–908.

O'Day CL, Dalbadie-McFarland G, Abelson J. 1996. The *S. cerevisiae* Prp5 protein has RNA-dependent ATPase activity with specificity for U2 snRNA. *J Biol Chem 271*:33261–33267.

Ono Y, Ohno M, Shimura Y. 1994. Identification of a putative RNA helicase (HRH1), a human homolog of yeast Prp22. *Mol Cell Biol 14*:7611–7620.

Patton JG, Porro EB, Galceran J, Tempst P, Nadal-Ginard B. 1993. Cloning and characterization of PSF, a novel pre-mRNA splicing factor. *Genes & Dev 7*:393–406.

Plumpton M, McGarvey M, Beggs JD. 1994. A dominant negative mutation in the conserved RNA helicase motif 'SAT' causes splicing factor PRP2 to stall in spliceosomes. *EMBO J 13*:879–887.

Raghunathan PL, Guthrie C. 1998. RNA unwinding in U4/U6 snRNPs requires ATP hydrolysis and the DEIH-box splicing factor Brr2. *Curr Biol 8*:847–855.

Reyes JL, Gustafson EH, Luo HR, Moore MJ, Konarska MM. 1999. The C-terminal region of hPrp8 interacts with the conserved GU dinucleotide at the 5′ splice site. *RNA 5*:167–179.

Reyes JL, Kois P, Konforti BB, Konarska MM. 1996. The canonical GU dinucleotide at the 5′ splice site is recognized by p220 of the U5 snRNP within the spliceosome. *RNA 2*:213–225.

Schägger H, von Jagow G. 1987. Tricine-sodium dodecyl sulfate-polyacrylamide gel electrophoresis for the separation of proteins in the range from 1 to 100 kDa. *Anal Biochem 166*:368–379.

Schmid SR, Linder P. 1992. D-E-A-D protein family of putative RNA helicases. *Mol Microbiol 6*:283–291.

Schwer B, Gross CH. 1998. Prp22, a DExH-box RNA helicase, plays two distinct roles in yeast pre-mRNA splicing. *EMBO J 17*:2086–2094.

Schwer B, Guthrie C. 1991. PRP16 is an RNA-dependent ATPase that interacts transiently with the spliceosome. *Nature 349*:494–499.

Schwer B, Guthrie C. 1992. A dominant negative mutation in a spliceosomal ATPase affects ATP hydrolysis but not binding to the spliceosome. *Mol Cell Biol 12*:3540–3547.

Sha M, Levy T, Kois P, Konarska MM. 1998. Probing of the spliceosome with site-specifically derivatized 5′ splice site RNA oligonucleotides. *RNA 4*:1069–1082.

Siatecka M, Reyes JL, Konarska MM. 1999. Functional interactions of Prp8 with both splice sites at the spliceosomal catalytic center. *Genes & Dev 13*:1983–1993.

Staley JP, Guthrie C. 1998. Mechanical devices of the spliceosome: Motors, clocks, springs, and things. *Cell 92*:315–326.

Staley JP, Guthrie C. 1999. An RNA switch at the 5′ splice site requires ATP and the DEAD box protein Prp28p. *Mol Cell 3*:55–64.

Strauss EJ, Guthrie C. 1991. A cold-sensitive mRNA splicing mutant is a member of the RNA helicase gene family. *Genes & Dev 5*:629–641.

Strauss EJ, Guthrie C. 1994. PRP28, a 'DEAD-box' protein, is required for the first step of mRNA splicing in vitro. *Nucleic Acids Res 22*:3187–3193.

Subramanya HS, Bird LE, Brannigan JA, Wigley DB. 1996. Crystal structure of a DExx box DNA helicase. *Nature 384*:379–383.

Tarn WY, Steitz JA. 1994. SR proteins can compensate for the loss of U1 snRNP functions in vitro. *Genes & Dev 8*:2704–2717.

Teigelkamp S, Mundt C, Achsel T, Will CL, Lührmann R. 1997. The human U5 snRNP-specific 100-kDa protein is an RS domain-containing, putative RNA helicase with significant homology to the yeast splicing factor Prp28p. *RNA 3*:1313–1326.

Velankar SS, Soultanas P, Dillingham MS, Subramanya HS, Wigley DB. 1999. Crystal structures of complexes of PcrA DNA helicase with a DNA substrate indicate an inchworm mechanism. *Cell 97*:75–84.

Vidal VP, Verdone L, Mayes AE, Beggs JD. 1999. Characterization of U6 snRNA–protein interactions. *RNA 5*:1470–1481.

Wagner JD, Jankowsky E, Company M, Pyle AM, Abelson JN. 1998. The DEAH-box protein Prp22 is an ATPase that mediates ATP-dependent mRNA release from the spliceosome and unwinds RNA duplexes. *EMBO J 17*:2926–2937.

Wang Y, Wagner JD, Guthrie C. 1998. The DEAH-box splicing factor Prp16 unwinds RNA duplexes in vitro. *Curr Biol 8*:441–451.

Wassarman DA, Steitz JA. 1992. Interactions of small nuclear RNA's with precursor messenger RNA during in vitro splicing. *Science 257*:1918–1925.

Yao N, Hesson T, Cable M, Hong Z, Kwong AD, Le HV, Weber PC. 1997. Structure of the hepatitis C virus RNA helicase domain. *Nat Struct Biol 4*:463–467.

Zhou Z, Reed R. 1998. Human homologs of yeast prp16 and prp17 reveal conservation of the mechanism for catalytic step II of pre-mRNA splicing. *EMBO J 17*:2095–2106.